Supplemental Information

Cytosolic carboxypeptidase 1 is involved in processing of α-tubulin and β-tubulin

Iryna Berezniuk[1], Hang T. Vu[2], Peter J. Lyons[3], Juan J. Sironi[3,4], Hui Xiao[5], Berta Burd[5], Mitsutoshi Setou[2], Ruth H. Angeletti[5], Koji Ikegami[2], and Lloyd D. Fricker[1,3]

1) Department of Neuroscience, Albert Einstein College of Medicine, Bronx, NY 10461
2) Department of Cell Biology and Anatomy, Hamamatsu University School of Medicine, 1-20-1 Handayama, Hamamatsu 431-3192, Japan
3) Department of Molecular Pharmacology, Albert Einstein College of Medicine, Bronx, NY 10461
4) Department of Pathology, Albert Einstein College of Medicine, Bronx, NY 10461
5) Laboratory of Macromolecular Analysis and Proteomics, Albert Einstein College of Medicine, Bronx, NY 10461

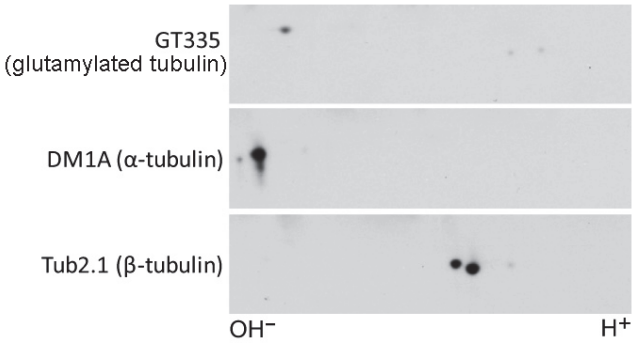

Figure S1. Levels of polyE tubulins in HEK293T cells. Cell lysates of HEK293T cells were subjected to high-resolution 2DE. There are almost no poly-glutamylated tubulins.

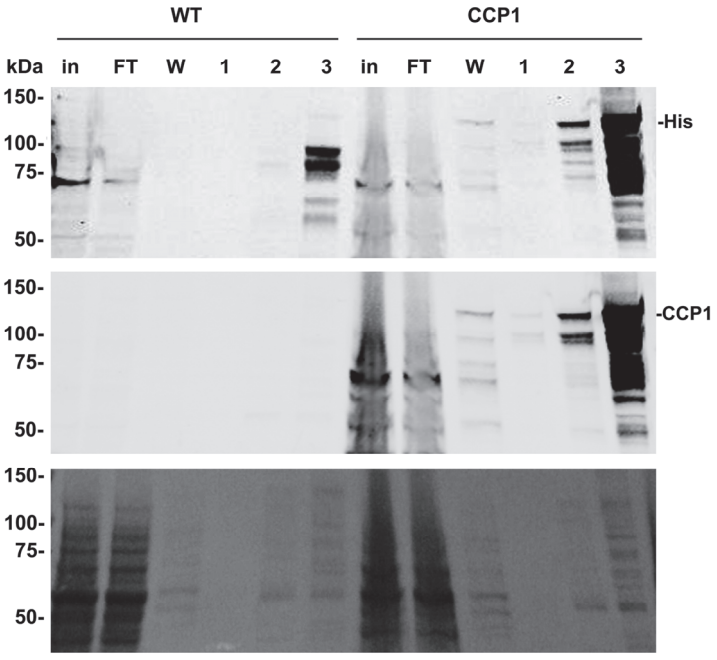

Figure S2. Purification of recombinant CCP1. Immunoblot analysis of fractions obtained during purification. Sf9 cells were infected with WT or His-tagged CCP1 recombinant baculovirus. Cell extracts (input, in) were loaded into the Talon column and non-bound fraction (flow-through, FT), wash (W), elute with 10 mM imidazole (1), elute with 20 mM imidazole (2), and elute with 80 mM imidazole (3) were collected. Aliquots of fractions (0.1% of in and FT, 1% of other fractions) were separated by SDS-PAGE and either probed with tetra-His antibody (upper panel), CCP1 antisera (middle panel) or stained with ponceau S solution (lower panel). The theoretical MW of CCP1 is 130 kDa.

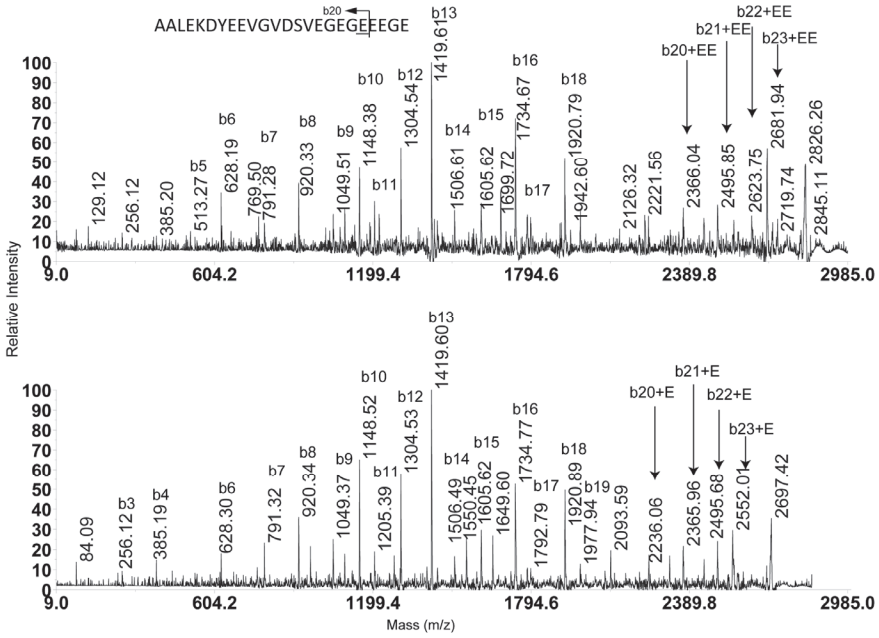

Figure S3A. Fragmentation profiles of the C-terminal representative peptides from α-tubulin. (Top) Positive MALDI TOF-TOF MS/MS spectrum of the precursor 2696.2 of α1a/α1b/α3. (Bottom) Positive MALDI TOF-TOF MS/MS spectrum of the precursor 2825.3 of α1a/α1b/α3. Each of the sequence is shown in the figures. Mainly b ions are labelled in the mass spectra. The polyglutamylated site of both peptides is underlined.

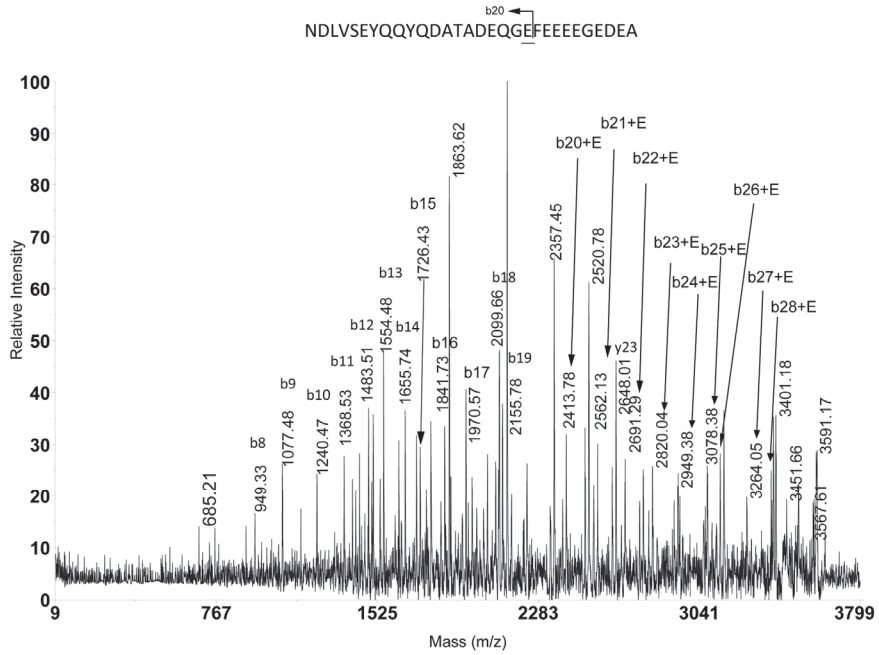

Figure S3B. Fragmentation profiles of the C-terminal representative peptides from β-tubulin. Positive MALDI TOF-TOF MS/MS spectrum of the precursor 3595.8 of β2b. Each of the sequence is shown in the figures. Mainly b ions are labelled in the mass spectra. The polyglutamylated site of both peptides is underlined.

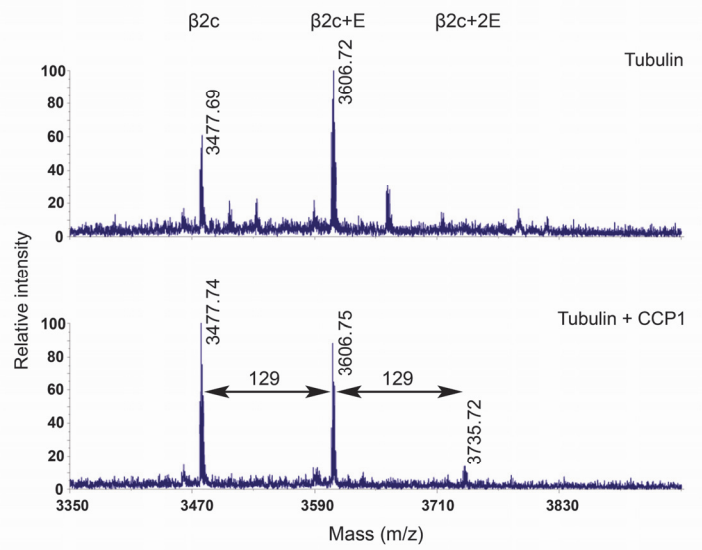

Figure S4. β2c tubulin isoform processing by purified CCP1. Representative spectra of β2c form of porcine β-tubulin. After incubation, tubulin was isolated on polyacrylamide gel, digested with CNBr, and analyzed as described. The form shown is the C-terminal region of β2c.**Top panel:** spectrum of β2c brain tubulin alone. **Bottom panel:** spectrum of β2c brain tubulin after incubation with purified CCP1. 129 is the molecular weight of Glu residue in Da.

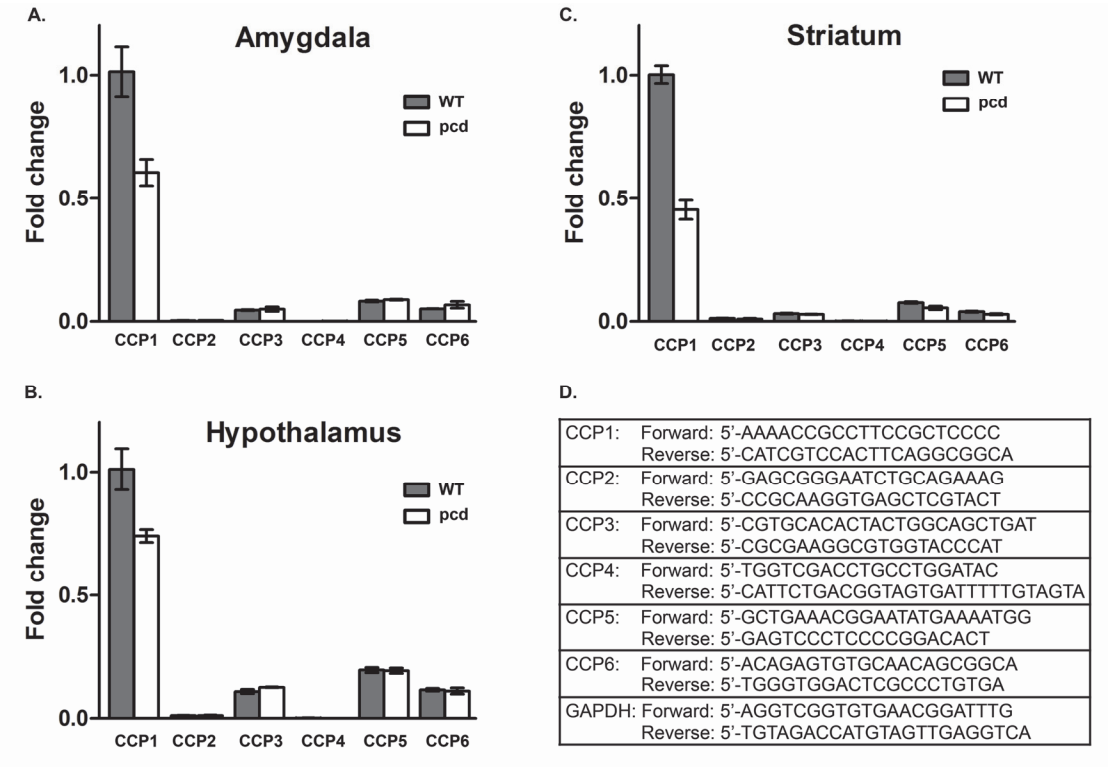

CCP1:	Forward: 5'-AAAACCGCCTTCCGCTCCCC Reverse: 5'-CATCGTCCACTTCAGGCGGCA
CCP2:	Forward: 5'-GAGCGGGAATCTGCAGAAAG Reverse: 5'-CCGCAAGGTGAGCTCGTACT
CCP3:	Forward: 5'-CGTGCACACTACTGGCAGCTGAT Reverse: 5'-CGCGAAGGCGTGGTACCCAT
CCP4:	Forward: 5'-TGGTCGACCTGCCTGGATAC Reverse: 5'-CATTCTGACGGTAGTGATTTTTGTAGTA
CCP5:	Forward: 5'-GCTGAAACGGAATATGAAAATGG Reverse: 5'-GAGTCCCTCCCCGGACACT
CCP6:	Forward: 5'-ACAGAGTGTGCAACAGCGGCA Reverse: 5'-TGGGTGGACTCGCCCTGTGA
GAPDH:	Forward: 5'-AGGTCGGTGTGAACGGATTTG Reverse: 5'-TGTAGACCATGTAGTTGAGGTCA

Figure S5. Relative levels of CCP mRNAs in the brain of wild-type and *pcd* mice. Quantitative real-time PCR was performed to determine mRNA levels of CCP1through 6 in amygdala, hypothalamus, and striatum (panels **A**, **B**, and **C**, respectively) of adult wild-type and mutant mice. CCP1 mRNA is the most abundant among other CCP mRNAs in wild-type mice. The levels of CCP1 mRNA are lower in *pcd* mice, but the levels of other CCP transcripts are not affected by CCP1 mutation. **D:** Mouse primers used for quantitative real-time PCR. Fold change in expression was calculated using the DDCt method. GAPDH was used as an internal control. n = 4 (wild-type), n = 2 (*pcd*).

Table S1. Primers used for Quantitative real-time PCR of human cell lines.

CCP1	Forward: 5'-GCAGTGAAGCGTTTACCCT Reverse: 5'-GCTGGGGCGATATGGCTC
CCP2	Forward: 5'-GGGAGGCAAACGAGGAAT Reverse: 5'-CTGCCCATCATCCGTGT
CCP3	Forward: 5'-GCTAGGGAGATGGGTGCC Reverse: 5'-AGGGGTTCCGTTTCTAAGCC
CCP4	Forward: 5'-GATATTCGGAGGCTCATCCA Reverse: 5'-CTGCATACCGCTCACTTTGA
CCP5	Forward: 5'-GAGCACAGCAGCCTTACT Reverse: 5'-GCAACCCATTGTGACTTT
CCP6	Forward: 5'-TTCCTATTGCTACACCCT Reverse: 5'-CACCTTTTCAACCACG
GAPDH	Forward: 5'-GAAGGTGAAGGTCGGAGT Reverse: 5'-GAAGATGGTGATGGGATTTC

Movie S1. Athletic performance of *pcd*/Δ*Ttll1* mouse.
The *pcd*/Δ*TTll1* mouse was made to grasp a cord with the body on the downside of the cord. The mouse climbed onto the cord within a few seconds.

Movie S2. Athletic performance of *pcd* mouse.
The *pcd* mouse was made to grasp a cord with the body on the downside of the cord. The mouse failed to climb onto the cord within the allotted time of 1 minute.

Movie S3. Comparison of athletic performance of *pcd* mouse with *pcd*/Δ*Ttll1* and wild-type mice.
The movie shows the severe ataxia of *pcd* mouse compared with *pcd*/Δ*Ttll1* and wild-type mice.